THE ASTRONOMICAL JOURNAL VOLUME 107, NUMBER 1 JANUARY 1994

HEAT FROM PLUTO

DAVID C. JEWITT[1]
Institute for Astronomy, 2680 Woodlawn Drive, Honolulu, Hawaii 96822
Electronic mail: jewitt@hubble.ifa.hawaii.edu

Received 1993 June 23; revised 1993 September 7

ABSTRACT

Submillimeter photometry from the James Clerk Maxwell Telescope on Mauna Kea is used to study thermal emission from Pluto. The brightness temperatures at 800 and 1300 μm are $T_B = 42 \pm 5$ K and $T_B = 35 \pm 9$ K, respectively, essentially confirming a prior measurement of $T_B = 39 \pm 3$ K at 1200 μm by Altenhoff *et al.* [A&A, 190, L15 (1988)]. These are substantially smaller than brightness temperatures obtained previously at 60 and 100 μm [Aumann & Walker, AJ, 94, 1088 (1987); Sykes *et al.*, Science, 237, 1336 (1987)], showing that the surface of Pluto is nonisothermal, nongrey, or both. The data are incompatible with nitrogen-covered, isothermal $T \sim 35$ K Pluto models [Owen *et al.*, Science, 261, 745 (1993)]. We suggest that the surface may be divided into cold regions coated by nitrogen ice plus warmer regions devoid of nitrogen, and we tentatively identify the latter with optically dark patches on Pluto's surface.

1. INTRODUCTION

A dramatic surge of scientific interest in the outermost known planet, Pluto, has occurred in the last 15 years. In large part, this surge has been driven by (1) the discovery of Pluto's satellite, Charon (Christy & Harrington 1978), 2) the spectroscopic detection of methane on Pluto (Cruikshank *et al.* 1976; Fink *et al.* 1980) and hence the inference of a possible atmosphere, (3) the unveiling of the dimensions and gross optical characteristics of the Pluto–Charon pair from mutual event observations (e.g., Tholen & Buie 1988; Buie *et al.* 1992; Young & Binzel 1993), and (4) the unambiguous detection of an atmosphere (Elliot *et al.* 1989). Very recently, solid nitrogen has been identified as the dominant surface ice, and nitrogen is inferred as the dominant atmospheric constituent (Owen *et al.* 1993).

Largely as a result of the above studies, many of the physical parameters of Pluto are now known with impressive accuracy: an exhaustive summary has been given by Stern (1992). One key variable that is not well known is the surface temperature. The temperature is of paramount importance in controlling the physical state of surface volatiles on Pluto, and has a decisive influence on the surface pressure and structure of the lower atmosphere (cf. Trafton & Stern 1983; Eshleman 1989). Sublimation of nitrogen ice is expected to buffer the surface temperature, leading to a surface that is isothermal and to an atmosphere whose pressure is directly connected to the surface temperature. For instance, a buffered nitrogen atmosphere would have pressure $P \sim 6200$ N m^{-2} (62 mbar) at $T = 60$ K, falling to $P \sim 5.7$ N m^{-2} (57 μbar) at $T = 40$ K (Brown & Ziegler 1980). Thus, it is of considerable interest to know the surface temperature on Pluto.

Measurements of 60 and 100 μm radiation by *IRAS* were used to derive subsolar temperatures on Pluto and Charon $T_{SS} \sim 59$ K (Sykes *et al.* 1987) under particular *assumed* values for the emissivity, infrared beaming factor, and albedo. This high temperature would imply a substantial atmosphere due to sublimation of N_2 with surface pressure $P \sim 50$ mbar. *IRAS* "survey" measurements (Tedesco *et al.* 1987) gave flux densities ($S_{60} \sim 420 \pm 40$ mJy) that are rather smaller than, but statistically consistent with, measurements from *IRAS* "pointed" observations ($S_{60} \sim 581 \pm 58$ mJy; Sykes *et al.* 1987). The difference, if real, may result from rotation of the Pluto–Charon pair. Using the same *IRAS* data, Aumann & Walker (1987) found acceptable fits with Pluto temperatures in the range 45 to 58 K. The lower temperatures in this range are artifacts of the adoption of Pluto and Charon radii that are larger than now considered acceptable.

Earlier measurements at 1200 μm (Altenhoff *et al.* 1988) were also interpreted using values of the Pluto and Charon diameters that are now known to be incorrect. In addition, a small pointing error in the Altenhoff *et al.* data raised doubts about the measurement in the minds of some researchers, although Altenhoff (1992) has subsequently confirmed it. An independent 3σ measurement of Pluto at 1100 μm was reported by Stern & Weintraub (1992). The accuracy of this measurement is too low to usefully constrain the Pluto surface temperature and we do not consider it further here. Very recent, more accurate measurements by Stern *et al.* (1993) are discussed in the context of the present work in Sec. 4.

In this paper, we present independent observations of

[1]Visiting Astronomer at the James Clerk Maxwell Telescope, operated by the Royal Observatory Edinburgh on behalf of the Science and Engineering Research Council of the United Kingdom, the Netherlands Organisation for Scientific Research, and the National Research Council of Canada.

 0004-6256/94/107(1)/372/7/$0.90

Pluto–Charon at 800 and 1300 μm wavelengths and attempt to use them to constrain the surface temperature.

2. OBSERVATIONS

The present observations were taken at the $f/35$ Nasmyth focus of the 15 m diameter James Clerk Maxwell Telescope (JCMT) on Mauna Kea, Hawaii. We used the He^3 cooled Germanium bolometer "UKT14" (Duncan *et al.* 1990). This is a single-element detector which views a patch of sky defined by a circular diaphragm 65 mm in diameter corresponding to 18 arcsec at 800 μm. The measurements therefore refer to the combined radiation from Pluto and Charon (apparent separation $\leqslant 1$ arcsec). Observations were taken using broadband filters centered at 800 and 1300 μm, both having fractional widths $\Delta\lambda/\lambda \sim 0.25$ (see Duncan *et al.* 1990 for the filter transmission curves). Observations at 800 μm were taken UT 1992 May 2.40–2.48 and May 3.40–3.47, while those at 1300 μm were taken UT 1992 May 4.35–4.47.

The accuracy of the Pluto photometry is determined primarily by the ability to subtract the bright submillimeter sky background. Sky subtraction was obtained by chopping the JCMT beam 60 arcsec in azimuth at a frequency of 7.8 Hz. In addition, the telescope was nodded in azimuth at 0.1 Hz, so as to eliminate residual imbalance between the object and sky beams. Observations of blank sky always gave net signals consistent with zero, confirming the accuracy of the sky cancellation techniques. The JCMT was tracked at nonsidereal rates in order to follow the motion of Pluto with respect to the fixed stars. Absolute pointing of the JCMT during the Pluto observations was determined by offsets from nearby sources of well known position (namely 1413+135 and 16293−2422). Positional measurements were repeated approximately every 45 min, and showed that the pointing was accurate to ± 1 arcsec rms, corresponding to a small fraction of the 18 arcsec beam.

Pluto was observed at airmasses in the range 1.0 to 1.2 on nights when the zenith optical depth at 1300 μm was 0.06 or better. Photometric calibration of the data was obtained using observations of nearby objects of known flux density. Primary photometric calibrations were taken from Jupiter (Griffin *et al.* 1986). The flux calibration of Jupiter was independently checked against IRC +10 216 (Sandell 1993), which was itself calibrated against Mars, Uranus, and Neptune (Orton *et al.* 1986). The independent cross checks were consistent to $\pm 5\%$. Uncertainties in the models used to predict the absolute Mars and gas-giant flux densities are probably of similar size. The adopted flux densities of the main calibration sources are listed in Table 1, while geometric and physical parameters of Pluto–Charon at the times of observation are listed in Table 2.

TABLE 1. Calibration sources.

Source	Date	S_{800} [Jy]	S_{1300} [Jy]
Jupiter	1992 May	4.97×10^3	2.70×10^3
Jupiter	1992 Aug	4.60×10^3	2.37×10^3
Uranus	1992 Aug	8.60×10^1	4.15×10^1
Neptune	1992 Aug	3.06×10^1	1.45×10^1
IRC +10 216	1992 May	5.98±0.44	

3. RESULTS

The Pluto measurements are summarized in Table 3, together with significant detections (3σ or greater) from the literature. There it may be seen that we obtained a combined 6.4σ measurement of Pluto at 800 μm and a 3.2σ measurement at 1300 μm. We obtained mutually consistent flux densities $S_{800}=31.3\pm 10.1$ mJy on UT 1992 May 2.44 and $S_{800}=43.4\pm 7.6$ mJy on UT 1992 May 3.44. The spectral index in the 800 to 1300 μm range is

$$\alpha = -d \ln S_\nu / d \ln \lambda = 2.3 \pm 0.3, \quad (1)$$

consistent with Rayleigh–Jeans emission ($\alpha=2$) from an isothermal source. The brightness temperatures (temperature of a blackbody radiator having the same dimensions and location as Pluto) are $T_B(800\ \mu\text{m})=42\pm 5$ K and $T_B(1300\ \mu\text{m})=35\pm 9$ K, while the weighted mean brightness temperature is $T_B=40\pm 4$ K.

For comparison, the flux density measured at 1200 μm by Altenhoff *et al.* (1988) is reinterpreted using Pluto and Charon radii 1151 and 593 km, respectively (Tholen & Buie 1988). Slightly larger radii derived from occultation data (cf. Millis *et al.* 1993) lead to temperatures that are smaller by 2 to 4 K. The 1200 μm measurement corresponds to a brightness temperature $T_B=39\pm 3$ K, where the quoted standard deviation ignores absolute calibration errors in the 1200 μm photometry. This is remarkably consistent with the brightness temperatures at 800 and 1300 μm (see Table 3). In turn, this consistency suggests that the pointing error described by Altenhoff *et al.* (1988) was indeed fully corrected, as these authors claimed.

After submission of this paper to *The Astronomical Journal*, we received two related preprints by FAX. Stern *et al.* (1993) give an improved 800 μm flux density, based on data from UT 1993 Jan 26.8. This flux density, $S_{800}=33\pm 7$ mJy, is statistically consistent with the value obtained here, and corresponds to a brightness temperature $T_B=40\pm 6$ K. They further report $S_{1300}=15\pm 5$ mJy on UT 1993 May 22. Both brightness temperatures are compatible with the Altenhoff data and with the data presented here. The preprint by Sykes (1993) reexamines the *IRAS* 60 and 100 μm flux densities, and offers an abbreviated discussion along the lines of the one given in Sec. 4.

TABLE 2. Physical parameters.

Object	R [AU]	Δ [AU]	α [deg]	r [km]	P [days]	p_b
Pluto	29.70	28.74	-0.6	1151	6.39	0.4 - 0.6
Charon	29.70	28.74	-0.6	593	6.39	0.38

TABLE 3. Pluto photometry.

Date	R [AU]	Δ [AU]	λ [μm]	S_ν [mJy]	T_B [K]	Reference
July 1983	29.88	29.80	60	420 ± 40[1]	51 ± 1	Tedesco *et al.* (1987)
Aug 1983	29.87	30.28	60	581 ± 58	55 ± 1	Sykes *et al.* (1987)
	29.87	30.28	100	721 ± 123	54 ± 3	
May 1992	29.70	28.74	800	39 ± 6	42 ± 5	This work
Feb-Apr 1986	29.73	28.78	1200	17.4 ± 1.6	39 ± 3	Altenhoff *et al.* (1988)
May 1992	29.70	28.74	1300	13 ± 4	35 ± 9	This work
Jan 1993	29.72	30.02	800	33 ± 7	40 ± 6	Stern *et al.* (1993)
May 1993	29.74	28.77	1300	15 ± 5	40 ± 11	Stern *et al.* (1993)

Notes to Table 3

[1] A small (< 1σ) adjustment to this flux density is suggested by Sykes (1993).

4. DISCUSSION

We seek to interpret the measured flux densities in terms of the surface temperature on Pluto. The observation that the brightness temperature at *IRAS* wavelengths is higher than at submillimeter wavelengths (Table 3) shows immediately that thermal emission from Pluto–Charon is nonisothermal, nongrey, or both. A lower limit to the allowed disk-averaged surface temperature is given by the submillimeter data. Within the uncertainties, the brightness temperatures from independent measurements at 800, 1200, and 1300 μm (Table 3) are consistent with the weighted mean $T_B = 39 \pm 3$ K. This would equal the physical temperature of the surface if the submillimeter emissivity were unity. Since the emissivity must be less than unity for any real material, we may regard $T_B = 39 \pm 3$ K as a practical lower limit to the physical temperature at the surface. Higher temperatures are required if the submillimeter emissivity is less than unity, and are necessary to fit the *IRAS* data.

For our present purposes, we scale all flux densities to the heliocentric and geocentric distances $R = 29.70$ AU and $\Delta = 28.73$ AU. The flux density received at Earth is

$$S_\nu = \int_{\Omega_p} \varepsilon_{\nu,p} B_\nu[T_p(\theta,\phi)]\, d\Omega_p + \int_{\Omega_c} \varepsilon_{\nu,c} B_\nu[T_c(\theta,\phi)]\, d\Omega_c, \quad (2)$$

where subscript "p" denotes Pluto and "c" denotes Charon, ε_ν is the emissivity of the surface at frequency ν[Hz], B_ν[W m^{-2} Hz^{-1} sr^{-1}] is the Planck function and the integration for solid angle, Ω, extends over all elements of the surface visible to the observer. In general, the temperature, T (θ,ϕ) [K], is a function of position on the surface, here specified by the polar angles θ,ϕ. Clearly, Eq. (2) contains too many unknowns for us to obtain a unique solution for the surface temperature and its spatial variation. Nevertheless, we can use the equation and the photometry to constrain ranges of plausible solutions, and to identify some others which are at variance with the observations.

4.1 Uncertainties

There are four principal sources of uncertainty in the interpretation of the thermal observations through Eq. (2).

(1) The vertical variation of temperature in the surface, $T(z)$. We assume that the submillimeter wavelengths sample a range of depths in the surface that is small compared to the vertical scale of the diurnal thermal wave. In other words, the emitting volume is taken to be vertically isothermal, $T(z) =$ constant. The vertical scale of the diurnal thermal wave is given by $z_{th} \sim (P\kappa)^{1/2}$, where $P = 6.39$ days is the rotation period of Pluto (e.g., Tholen & Buie 1988) and κ[m^2 s^{-1}] is the thermal diffusivity of the surface material. With $\kappa \sim 10^{-6}$ m^2 s^{-1}, we find $z_{th} \sim 0.7$ m, or $z_{th} \sim 700\lambda$. For comparison, common dielectrics have absorption lengths $\sim 10\lambda$ in the microwave (Campbell & Ulrichs 1969). Although we do not possess laboratory determinations of the absorption lengths for nitrogen ice at $\lambda \sim 1$ mm, it seems likely that the millimeter wavelengths are emitted from a surface skin that is thin compared to z_{th} and which is therefore vertically isothermal. The submillimeter spectral index $\alpha \sim 2$ lends support to this assumption. Rotational variations are, in any case, muted by the low cooling rates at the large heliocentric distance of Pluto (cf. Spencer *et al.* 1989).

(2) The value of the submillimeter emissivity of the surface, ε_ν. The submillimeter emissivity of solid nitrogen is unknown, as is its wavelength dependence. Naively, we might expect that the emissivity should be substantially less than unity, since N_2 lacks strong rotational and vibrational features near $\lambda \sim 1$ mm. The emissivity might also be changed by the CH_4 and CO trace constituents spectroscopically detected by Owen *et al.* (1993). In the absence of laboratory data, we can only assume $\epsilon_\nu \leqslant 1$.

(3) Thermal emission from Charon contaminates the signal due to Pluto. Fortunately, the radius and geometric albedo of Charon are relatively well known, allowing us to compute and subtract its emission (see below). The ratio of the geometric cross section of Charon to the total cross section (Charon+Pluto) is 0.21 (Tholen & Buie 1988). Charon has a blue geometric albedo (0.38) that is smaller than that of Pluto (0.44–0.61), and hence may possess a slightly higher surface temperature (Tholen & Buie 1988; Buie *et al.* 1993). However, at long wavelengths, the emitted flux density is weakly dependent on the temperature, so that we expect the fractional contribution of Charon to the submillimeter photometry to be of order 0.21.

In the remainder of this paper, we have adopted a "latitude-isothermal" model of Charon, in which the temperature is constant at a given latitude. This temperature distribution is appropriate on distant rotating objects when the time scale for radiation cooling of the diurnal surface skin is longer than the rotation period (Spencer *et al.* 1989; Sykes *et al.* 1987). The temperature at latitude θ is $T_c(\theta) = T_c(0)\cos^{1/4}\theta$, where $T_c(0)$ is the subsolar temperature given by

$$T_c(0) = \left[\frac{F_{Sun}(1-A)}{R^2 \pi \sigma \varepsilon}\right]^{1/4}. \quad (3)$$

Here, $F_{Sun}=1360$ W m^{-2} is the solar constant, $A\sim0.18$ the Bond Albedo, R the heliocentric distance in AU, $\sigma=5.67\times10^{-8}$ W m^{-2} K^{-4} is the Stefan Constant and $\epsilon\sim0.9$ the emissivity near the peak of the emission spectrum. We employ $T_c(0)=53$ K for the calculations here, based on optical parameters from Tholen & Buie 1988 (see also Sykes *et al.* 1987). Note that, since Charon contributes a small fraction of the total flux, our conclusions about Pluto are not strongly dependent on $T_c(0)$ or on the adoption of the latitude-isothermal model.

(4) The form of the temperature distribution on the surface of Pluto, $T_p(\theta,\phi)$, is uncertain. In the absence of an atmosphere, the latitude-isothermal model already adopted for Charon would apply to Pluto with equal validity. The presence of albedo spots on Pluto would render a more complex temperature distribution. Conversely, latent-heat buffering by nitrogen sublimation would tend to produce a surface that is isothermal (Trafton & Stern 1983; Owen *et al.* 1993).

4.2 Isothermal Models

We first consider an isothermal Pluto, $T_p(\theta,\phi)=T_p=$constant, such as would be obtained in a heavily buffered atmosphere produced by sublimation of surface volatiles (Trafton & Stern 1983; Owen *et al.* 1993). In this case, the flux density from Pluto is simply

$$S_{\nu,p}=\epsilon_{\nu,p}B_\nu(T_p)\Omega_p, \quad (4)$$

where $T_p=$constant and Ω_p is the solid angle subtended by Pluto. Note that Eq. (4) gives an observational constraint on the product $\epsilon_\nu B_\nu(T_p)$, but not on the emissivity or the temperature separately. Thus, measurements of thermal emission cannot be used to uniquely determine either the emissivity or the temperature. Examples of grey ($\epsilon_\nu=1$), isothermal Pluto models are shown in Fig. 1.

We find no acceptable isothermal greybody fits to the combined *IRAS* (60 and 100 μm) and submillimeter (800 to 1300 μm) measurements. The $T_p=55$ K isotherm fits the 60 and 100 μm data but predicts flux densities at 800, 1200, and 1300 μm that are systematically too high by factors 1.4 ± 0.2, 1.5 ± 0.1, and 1.7 ± 0.4, respectively. Isothermal models with $T_p=35$ K, as suggested by Owen *et al.* (1993), are compatible with the submillimeter data considered alone, but predict flux densities at 60 and 100 μm that are several times too small to match the *IRAS* data.

Better agreement can be achieved using a nongrey, isothermal model in which the emissivity decreases linearly from $\epsilon=0.9$ at 20 μm to $\epsilon=0.5$ at 1500 μm (Fig. 2). The best-fit temperature in this case is $T_p=55\pm5$ K. This form of the emissivity is completely arbitrary. Nevertheless, it serves to show that all isothermal, nongrey models require surface temperatures higher than 35 K.

Greybody, latitude-isothermal Pluto models provide a marginally better fit to the combined data than do the isothermal models. This improved fit is a result of the equator-to-pole temperature gradient, which partially compensates for the elevated flux densities measured at short wavelengths on Pluto. However, we still find no acceptable greybody fits to the *IRAS*-submillimeter thermal data when using latitude-isothermal models.

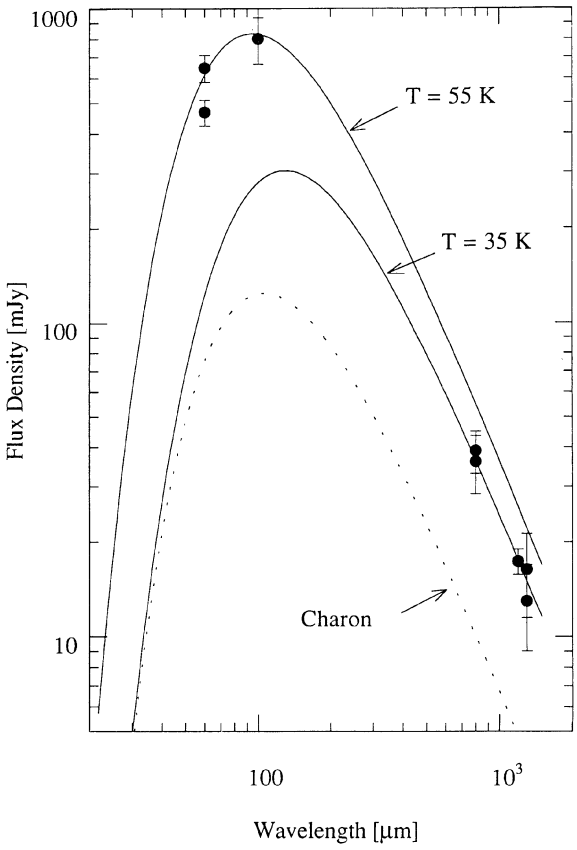

FIG. 1. Isothermal, blackbody Pluto models are plotted with the data from Table 3. The models show emission from isothermal Plutos at temperatures $T=35$ K and $T=55$ K, as marked. Solid lines denote the total emission from Pluto and Charon. Emission from Charon is shown separately: it is a small fraction of the total emission at all wavelengths $\lambda>50$ μm. No isothermal, greybody models are able to match both the *IRAS* and submillimeter observations.

4.3 Two-Temperature Models

Synthesized albedo maps of Pluto at $\sim$450 km resolution show surface regions with albedos in the approximate range 0.2 to 1.0 (Buie & Tholen 1992; Young & Binzel 1993). Viewed at higher resolution, the local albedo contrasts might be still more extreme. Presumably, these albedo variations reflect differences in the amount or purity of surface frosts and snows. If the optically dark regions are dirty nitrogen ice, then we would expect no corresponding temperature differences, since the sublimation buffer will come into effect. However, if the dark regions are free of nitrogen ice, we would expect surface temperature variations to result from the albedo differences.

Accordingly, we consider a two-temperature model in which a fraction, f, of the surface of Pluto is hot (temperature T_{high}) while the remaining surface has a lower tem-

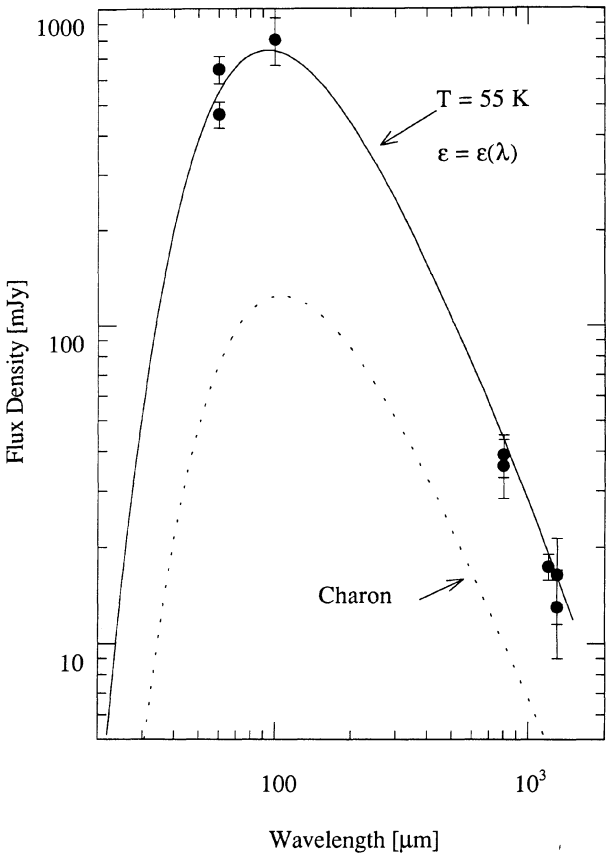

FIG. 2. Sample nongrey, isothermal Pluto model in which the emissivity decreases linearly from 0.9 at 20 μm to 0.5 at 1500 μm. A good fit to the combined *IRAS*/submillimeter observations is obtained. However, the assumed wavelength dependence of the emissivity is completely arbitrary. In all nongrey, isothermal models, surface temperatures substantially higher than 35 K are required to fit the *IRAS* data. Solid lines denote the total emission from Pluto and Charon. Emission from Charon is shown separately.

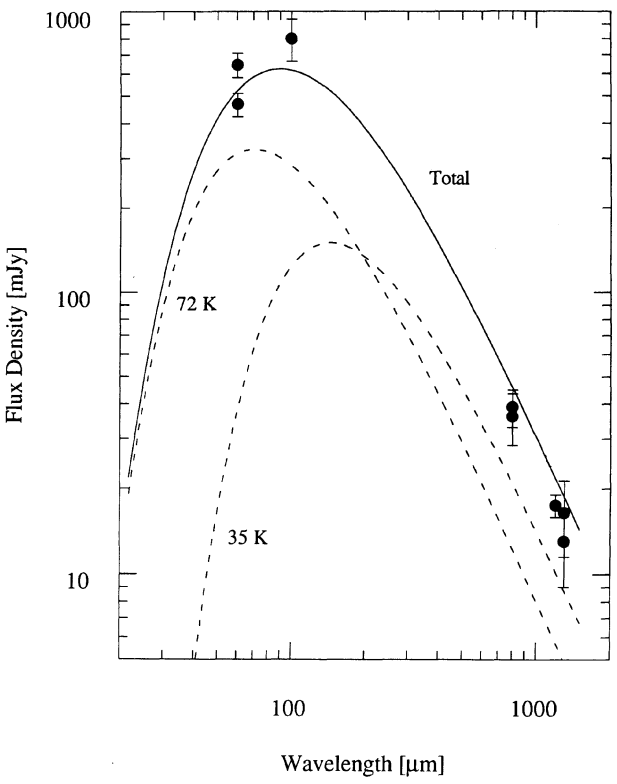

FIG. 3. Sample two-temperature model in which the surface of Pluto is divided into areas at temperatures $T_{high}=72$ K and $T_{low}=35$ K. Temperature T_{low} corresponds to areas of nitrogen ice in which low temperatures are sustained by sublimation (cf. Owen *et al.* 1993). Temperature T_{high} corresponds to regions free of nitrogen ice. Emissivity 1.0 is assumed throughout, and emission from Charon is included as described in the text. The plotted curves refer to a model in which the ratio of the hot area to the total area is 0.2. The separate contributions from the warm and cold areas are plotted with dashed lines.

perature T_{low}. The maximum conceivable passive surface temperature on Pluto is $T_{high}=72$ K, this being the temperature of a perfectly absorbing flat plate in instantaneous equilibrium with sunlight at the subsolar point. Higher temperatures could only be produced by active processes (e.g., volcanism), for which we have no evidence at present. In reality, planetary rotation will reduce the surface temperature *below* 72 K, but we employ this number as a limiting case. We further take $T_{low}=35$ K (the temperature of the N_2 sublimation-buffered surface estimated by Owen *et al.* 1993). For these particular choices of T_{high} and T_{low}, and for blackbody emission, we find a marginally acceptable fit to the combined 60–1300 μm data with $f\sim0.2$ (Fig. 3), meaning that $\frac{1}{5}$th of the surface of Pluto should be covered by the higher temperature material. The dotted curves in Fig. 3 show the separate contributions of the high and low temperature areas. Evidently, the high temperature material dominates the flux density at the *IRAS* wavelengths, while both high and low temperature areas contribute in the submillimeter. The fraction f is a strong inverse function of T_{high}, as may be seen in Table 4. Since $T_{high}=72$ K is a strong upper limit to the temperature of the warm regions, $f=0.2$ must be taken as lower limit to the fractional area of this material. No fit is obtained for $T_{high}<50$ K, because lower temperatures fail to produce flux densities sufficient to match the *IRAS* measurements.

TABLE 4. Two-temperature models.[1]

T_{high} [K]	f
72	0.2
70	0.3
65	0.4
60	0.55
55	0.8
50	>1

Notes to TABLE 4

[1] $T_{low}=35$ K is assumed.

We tentatively identify the warm areas with the optically dark albedo markings on Pluto (Buie & Tholen 1992; Young & Binzel 1993) and the cold, nitrogen-covered areas with the bright regions. The equatorial location of most of the dark markings is compatible with our requirement that they be free of solid nitrogen in order to avoid sublimation buffering of their temperature. However, the dark regions might contain other ices (e.g., water is a rock at Pluto temperatures) mixed with organic compounds analogous to those in the mantles of comets. Indeed, it is even possible that the dark markings represent lag deposits produced by sublimation of N_2 ice, in the same way that sublimation of water ice leaves behind refractory mantles on comets. If we accept that about 50% of the sun-facing hemisphere of Pluto is occupied by dark markings at any instant, then Table 4 shows that the dark material must be at temperature $T_{high} \sim 60$–65 K, safely below the limiting 72 K considered above. The warm, equatorial areas would heat the atmosphere and drive bulk motions, so that Pluto would support a complex circulation that could respond to seasons. Owen *et al.* (1993) remark that methane should quickly freeze out of the atmosphere if the global temperature is ~35 K, yet methane is required to sustain the observed atmospheric temperature at occultation levels [unless the Elliot *et al.* (1989) haze-layer model is correct]. The existence of warm areas might provide a natural source of atmospheric methane, reconciling the low nitrogen ice temperatures with the measured atmospheric structure.

In this interpretation, Pluto should exhibit a rotational thermal light curve that is anticorrelated with the optical light curve (since optically dark areas are thermally bright). Because of the exponential dependence of the Planck function on the temperature and wavelength, this rotational thermal light curve will be more apparent at *IRAS* wavelengths than in the submillimeter. The only way in which temperatures substantially in excess of 35 K on at least part of the surface can be avoided is if the *IRAS* measurements are somehow incorrect. While we have no specific reason to suspect an error in the *IRAS* data (cf. Sykes 1993), it would be most reassuring to obtain independent confirmation of the measurements at 60 and 100 μm. Such measurements could be attempted this decade using the ISO spacecraft.

Stern *et al.* (1993) lean in favor of low surface temperatures "probably near 35–37 K" and this temperature range is selected apparently to produce agreement with the temperature estimate by Owen *et al.* (1993). As described above, the nonuniqueness of the thermal problem allows room for a *fraction* of the surface of Pluto to be at these low temperatures, and in this sense our independent conclusions concur. However, low temperatures are not required by the thermal data, and *globally* low temperatures near 35–37 K are explicitly excluded by it. Nonisothermal solutions are independently considered by Sykes (1993).

Finally, we emphasize that all models presented here are nonunique, and necessarily oversimplify the Pluto–Charon system. Ideally, we should include wavelength dependence of the emissivity in the two-temperature models. In so doing, we could undoubtedly achieve "better" fits to the observations than those in Figs. 1–3, although the treatment of emissivity would be unavoidably arbitrary. To clarify the discussion, and to stress the weaknesses in the interpretation, we have kept temperature and emissivity effects separate. The outstanding problem in the thermal investigation of Pluto remains the unknown emissivity of solid nitrogen at long wavelengths. Laboratory measurements of the emissivity are thus an essential prerequisite for understanding the heat from this planet.

5. SUMMARY

(1) We measure submillimeter brightness temperatures of Pluto–Charon $T_B = 42 \pm 5$ K (at wavelength 800 μm) and $T_B = 35 \pm 9$ K (1300 μm) using the James Clerk Maxwell Telescope. These temperatures are in good agreement with $T_B = 39 \pm 3$ K (1200 μm) obtained by Altenhoff *et al.* (1988) when interpreted using modern values of the sizes of Pluto and Charon. They further agree with independent determinations $T_B = 40 \pm 6$ K (800 μm) and $T_B = 40 \pm 11$ K (1300 μm) by Stern *et al.* (1993). Thus, the submillimeter brightness temperatures of Pluto are observationally well determined.

(2) The submillimeter brightness temperatures are systematically smaller than brightness temperatures at 60 μm ($T_B = 55 \pm 1$ K) and 100 μm ($T_B = 54 \pm 1$ K) by Sykes *et al.* (1987) and Sykes (1993). This shows that the emission from Pluto is either nonisothermal, or nongrey, or both. The available data are specifically not compatible with an isothermal surface at 35 K, as has been proposed for Pluto by Owen *et al.* (1993).

(3) Our ability to specify the physical temperature on Pluto is fundamentally limited by the lack of knowledge of the emissivity of solid nitrogen frosts on its surface.

(4) Within this limitation, we find two families of models that are able to match the thermal emission data.

- First are models in which the emissivity is a strongly decreasing function of wavelength in the *IRAS* to submillimeter range. These models require uniform surface temperatures $T_p \sim 55 \pm 5$ K, and are again at variance with the low temperature (~35 K) inferred by Owen *et al.* 1993.
- Second are models in which the surface temperature is bimodally distributed. These models allow a fraction of the surface to be held at $T_{low} \sim 35$ K (nitrogen ice), while the remainder is at a higher temperature ($55 \leqslant T_{high} \leqslant 72$ K; nitrogen ice free). The fraction of the surface at T_{high} is uncertain, but is at least 20%. The warm areas are presumably free of solid nitrogen, and are tentatively identified with the optically dark, near-equatorial patches responsible for Pluto's rotational light curve.

I thank Kimberly Pisciotta and Jim Pomeroy for skillful operation of the JCMT, and Jim Annis and Jane Luu for assistance. Göran Sandell provided calibration information in advance of publication. Financial support from the planetary astronomy program of the National Science Foundation is greatly appreciated.

REFERENCES

Altenhoff, W. J. 1992, private communication
Altenhoff, W. J., Chini, R., Hein, H., Kreysa, E., Mezger, P. G., Salter, C., & Schraml, J. B. 1988, A&A, 190, L15
Aumann, H. H., & Walker, R. G. 1987, AJ, 94, 1088
Brown, G. N., & Ziegler, W. T. 1980, Adv. Cryog. Eng., 25, 662
Buie, M., Tholen, D. J., & Horne, K. 1992, Icarus, 97, 211
Campbell, M. J., & Ulrichs, J. 1969, J. Geophys. Res., 74, 5867
Christy, J. W., & Harrington, R. S. 1978, AJ, 83, 1005
Cruikshank, D. P., Pilcher, C. B., & Morrison, D. 1976, Science, 194, 835
Duncan, W. D., Robson, E. I., Ade, P. A. R., Griffin, M. J., & Sandell, G. 1990, MNRAS, 243, 126
Elliot, J. L., Dunham, E. W., Bosh, A. S., Slivan, S. M., Young, L. A., Wasserman, L. H., & Millis, R. L. 1989, Icarus, 77, 148
Eshleman, V. R. 1989, Icarus, 80, 439
Fink, U., Smith, B. A., Benner, D. C., Johnson, J. R., & Reitsema, H. J. 1980, Icarus, 44, 62
Griffin, M. J., Ade, P. A., Orton, G. S., Robson, E. I., Gear, W. K., Nolt, I. G., & Radostitz, J. V. 1986, Icarus, 65, 244
Millis, R. L., *et al.* 1993, Icarus (submitted)
Orton, G. S., Griffin, M. J., Ade, P. A., Nolt, I. G., Radostitz, J. V., Robson, E. I., & Gear, W. K. 1986, Icarus, 67, 289
Owen, T., *et al.* 1993, Science, 261, 745
Sandell, G. 1993, in preparation
Spencer, J. R., Lebofsky, L. A., & Sykes, M. V. 1989, Icarus, 78, 337
Stern, S. A. 1992, ARA&A, 30, 185
Stern, S. A, & Weintraub, D. A. 1992, BAAS, 24, 961
Stern, S. A., Weintraub, D. A., & Festou, M. C. 1993, Science, 261, 1713
Sykes, M. V. 1993, Science (submitted)
Sykes, M. V., Cutri, R. M., Lebofsky, L. A., & Binzel, R. P. 1987, Science, 237, 1336
Tedesco, E. F., Veeder, G. J., Dunbar, R. S., & Lebofsky, L. A. 1987, Nature, 327, 127
Tholen, D. J., & Buie, M. W. 1988, AJ, 96, 1977
Trafton, L., & Stern, S. A. 1983, ApJ, 267, 872
Young, E. F., & Binzel, R. P. 1993, Icarus, 102, 134